lysed with lysis buffer (10 mM Tris-HCl (pH 7.5), 10 mM NaCl, 0.5% NP-40). Internalized virion Gag p27 protein was measured using the SIV Core Antigen ELISA kit (Beckman Coulter).

Results

Comparison of viable cell counts after SIV infection

We could successfully establish $CD4^+$ and $CD4^+8^+$ T cell clones from monkey's PBMC by HVS-immortalized method (Fig. 1a). As shown in the right panel of Fig. 1a, the obtained $CD4^+8^+$ T cell clones appeared to contain two subpopulations, $CD4^{high}CD8^{high}$ T cells and $CD4^{high}CD8^{low}$ T cells. It is interesting to note that, when a single cell from either $CD4^{high}CD8^{high}$ or $CD4^{high}CD8^{low}$T cell clones was further cultured, those two promiscuous populations were always emerged. Therefore, the expression level of CD8 molecules on $CD4^+8^+$ T cells might fluctuate. Taking advantage of these $CD4^+$ T cell clones, we then examined their susceptibility to SIVmac239. SIVmac239-infected or uninfected T cells were plated in culture for 7 days and were estimated the viable cell counts by XTT colorimetric method. After 7 days of incubation, a total number of viable cells were significantly decreased in infected $CD4^+8^+$ T cells, whereas that was slightly decreased in infected $CD4^+$ T cells (Fig. 1b).

Assessment of viral replication in $CD4^+$ and $CD4^+8^+$ T cells

To determine viral protein production, the amount of p27 antigens and RT activity in the culture supernatants were measured. The supernatants from SIVmac239-infected $CD4^+8^+$ T cells contained large amounts of p27 antigens

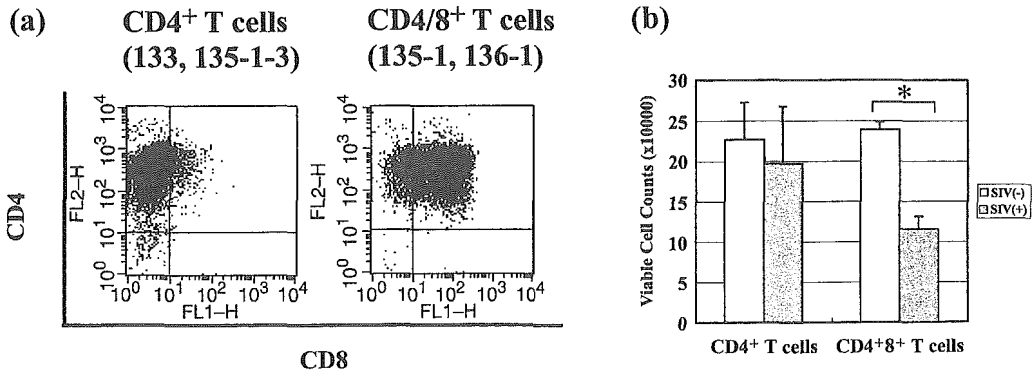

Fig. 1. a HVS-transformed $CD4^+$ and $CD4^+8^+$ T cells established from PBMC of rhesus macaques. Cells were stained with PE-labeled anti-CD4 mAb and FITC-labeled anti-CD8 mAb, followed by propidium iodide staining to exclude dead cells. **b** Determination of viable cell counts in $CD4^+$ and $CD4^+8^+$ T cells after SIV infection. Cells were inoculated with (□) or without (□) SIVmac239 (moi 0.5) and estimated the viable cells by XTT colorimetric method after 7 days incubation. The data shown are the mean of triplicate cultures ±SD (*$P < 0.01$)

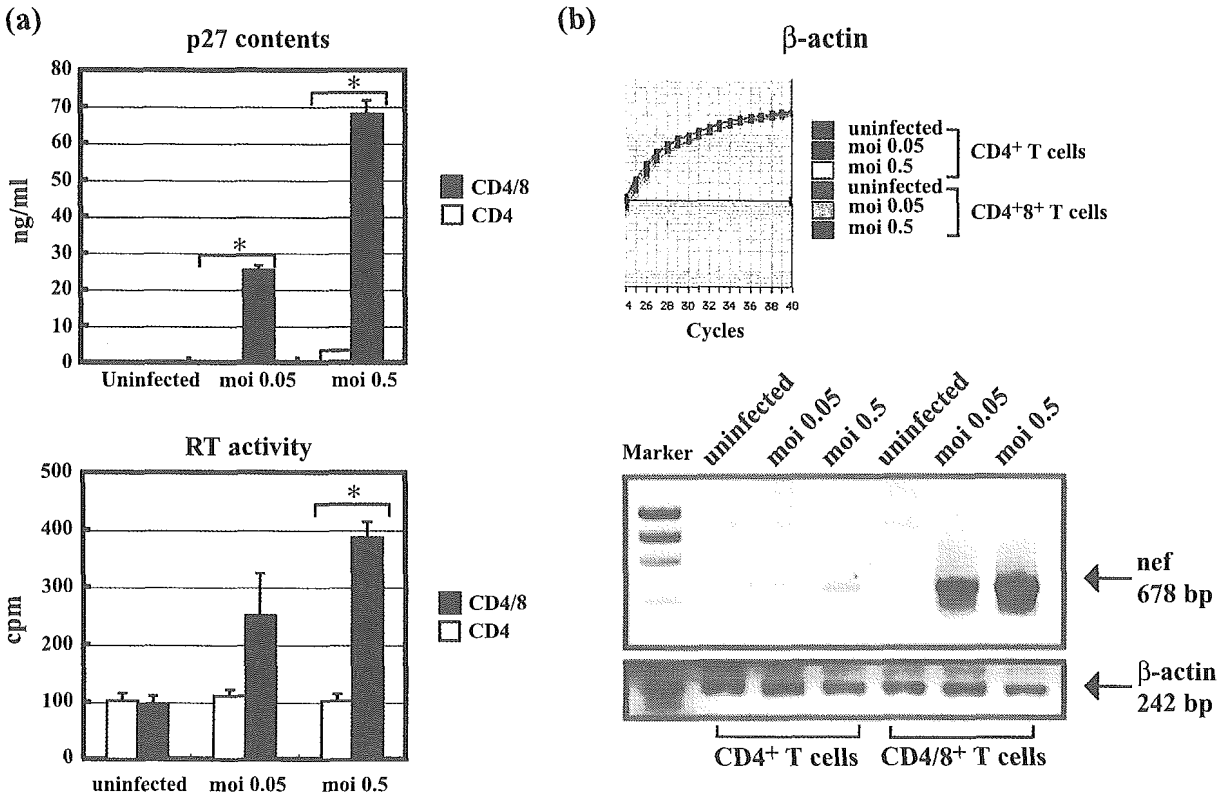

Fig. 2. Assessment of viral replication in $CD4^+$ and $CD4^+8^+$ T cells. $CD4^+$ (□) and $CD4^+8^+$ (■) T cells were infected with SIVmac239 (moi 0.05 or 0.5). After 4 days incubation; **a** the supernatants were harvested and subjected to measure the amount of p27 core antigen and RT activity. The data shown are the mean of triplicate cultures ±SD (*$P < 0.01$). **b** DNA was isolated from infected or uninfected cells and subjected to semi-quantitative PCR using SIVmac239 *nef* or β-actin primer. The thermal cycle was consisted of 30 s at 94 °C, 45 s at 60 °C for *nef* or 55 °C for β-actin, 45 s at 72 °C. The numbers of PCR cycles for *nef* were 35 cycles, and those of β-actin were 24 cycles to generate PCR products during the exponential phase of amplification

and higher level of the RT activity compared to that from infected $CD4^+$ T cells (Fig. 2a). Next, to determine the level of viral DNA synthesis in infected cells, we performed semi-quantitative PCR analysis using the primer pair for the *nef* gene of SIVmac239. As shown in Fig. 2b, low level of the *nef* DNA was detected in infected $CD4^+$ T cells, whereas an evident increase in the *nef* DNA was observed in infected $CD4^+8^+$ T cells.

Effect of SIV infection on CD3 and CD4 expression in $CD4^+$ and $CD4^+8^+$ T cells

It has been reported that HIV/SIV modulated the surface expression of various molecules [11]. Therefore, we analyzed the expression level of surface CD3 and CD4 molecules on both SIVmac239-infected $CD4^+$ and $CD4^+8^+$ T cells by

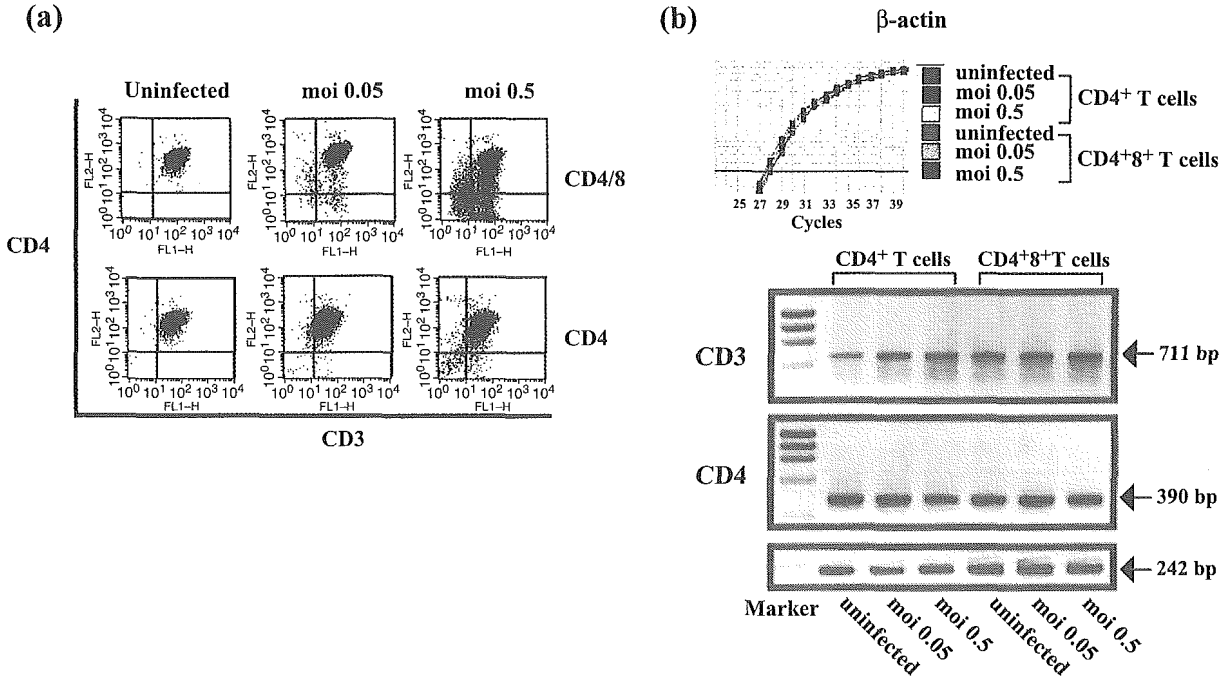

Fig. 3. Effect of SIVmac239 infection on CD3 and CD4 expression on $CD4^+$ and $CD4^+8^+$ T cells. $CD4^+$ and $CD4^+8^+$ T cells were infected with SIV (moi 0.05 or 0.5). After 4 days incubation; **a** Cells were stained with FITC-labeled anti-CD3 mAb and PE-labeled anti-CD4 mAb, followed by propidium iodide staining to exclude dead cells. **b** RNA was isolated from infected or uninfected cells and then reverse-transcribed into cDNA. cDNA was subjected to semi-quantitative PCR using CD3, CD4 or β-actin primer. The thermal cycle was consisted of 30 s at 94 °C, 45 s at 60 °C for CD3 and CD4, or 55 °C for β-actin, 45 s at 72 °C. The numbers of PCR cycles for CD3 and CD4 were 33 cycles, and those of β-actin were 24 cycles to generate PCR products during the exponential phase of amplification

flow cytometry. SIV-infected $CD4^+8^+$ T cells showed marked down-modulation for both CD3 and CD4 expression when compared with infected $CD4^+$ T cells (Fig. 3a). The down-modulation was dependent on the infectious doses of virus. Since semi-quantitative RT-PCR analysis demonstrated that the respective levels of CD3 and CD4 transcripts did not change between uninfected and infected cells, down-modulation is due to the internalization of these molecules induced by the virus infection (Fig. 3b).

Evaluation of receptor and co-receptor expression on $CD4^+$ and $CD4^+8^+$ T cells and virus entry

Since efficiency of SIV entry depends on the presence of appropriate receptor and co-receptor, we examined the expression levels of those receptors on uninfected $CD4^+$ T cells or $CD4^+8^+$ T cells by FACS and RT-PCR analysis. There seemed little difference in the expression levels of CD4, CXCR4 or CCR5. The transcript level of Bob was almost the same, whereas that of Bonzo was slightly decreased

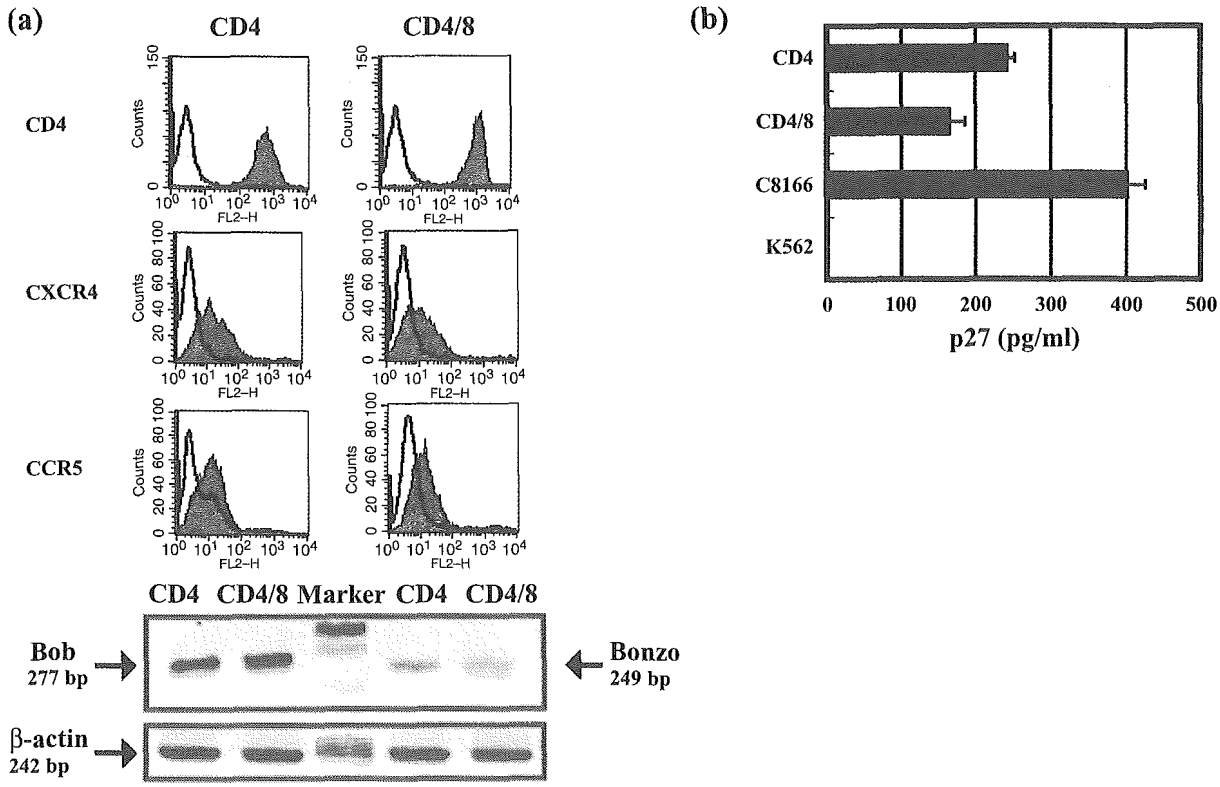

Fig. 4. Expression of receptor and co-receptor on $CD4^+$ and $CD4^+8^+$ T cells. **a** Uninfected cells were stained with PE-labeled anti-CD4 mAb, PE-labeled anti-CXCR4 mAb, or PE-labeled anti-CCR5 mAb, followed by propidium iodide staining to exclude dead cells. RNA was isolated from uninfected cells and then reverse-transcribed into cDNA. cDNA was subjected to semi-quantitative PCR using Bob, Bonso or β-actin primer. The thermal cycle consisted of 30 s at 94 °C, 45 s at 52 °C for Bob, 58 °C for Bonso or 55 °C for β-actin, 45 s at 72 °C. The numbers of PCR cycles for Bob and Bonso were 35 cycles, and those for β-actin were 24 cycles to generate PCR products during the exponential phase of amplification. **b** Entry efficiency of virus into $CD4^+$ and $CD4^+8^+$ T cells. Cells were incubated with virus (moi 1) for 2 h, followed by washing, trypsinizing, and lysed with lysis buffer. The p27 core antigen content in the lysate was monitored by ELISA. C8166 cells were used as positive control and K562 cells were used as negative one. The data shown are the mean of triplicate cultures ±SD

in $CD4^+8^+$ T cells (Fig. 4a). When we monitored the efficiency of virus entry into $CD4^+$ and $CD4^+8^+$ T cells at 2 h post-infection by the measurement of the intracellular p27 antigens, a slightly lower level of the amount of p27 antigens in $CD4^+8^+$ T cells was observed when compared with $CD4^+$ T cells (Fig. 4b). These observations indicate that the entry step of virus did not account for the increased amounts of virus accumulation in $CD4^+8^+$ T cells.

Efficiency of reverse transcription in $CD4^+$ and $CD4^+8^+$ T cells

To define at which step virus replication is accelerated in $CD4^+8^+$ T cells, we performed DNA-dependent PCR with primers that distinguish salient stages of

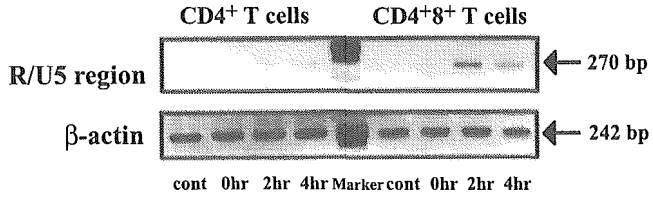

Fig. 5. Detection of the earliest reverse transcription product of SIV in $CD4^+$ and $CD4^+8^+$ T cells. DNA was isolated from infected or uninfected cells at indicated time and subjected to semi-quantitative PCR using R/U5 or β-actin primer. The thermal cycle consisted of 30 s at 94 °C, 45 s at 64 °C for R/U5 and 55 °C for β-actin, 45 s at 72 °C. The numbers of PCR cycles for R/U5 were 35 cycles, and those for β-actin were 25 cycles to generate PCR products during the exponential phase of amplification

reverse transcription. Cells were infected with SIV (moi 1) for 2 h. After washing to remove free virus, cells were further cultured and the genomic DNA was extracted from infected cells at 0, 2, and 4 h after incubation. The primer pair R/U5 can amplify the earliest reverse transcription product [1]. This earliest reverse transcription product was detected in both $CD4^+$ T cells and $CD4^+8^+$ T cells at 2 h after incubation, however, level of the product was higher in $CD4^+8^+$ T cells than in $CD4^+$ T cells (Fig. 5). Thus, after the entry of SIV, reverse transcription appeared to initiate more efficiently in $CD4^+8^+$ T cells than in $CD4^+$ T cells.

We speculated that some cellular components might act to function as an inhibitor or cofactor for viral reverse transcriptase in cells. We thus prepared the cell lysate from uninfected $CD4^+$ T cells or $CD4^+8^+$ T cells and performed RT assay in the presence of those cell lysate. In all cases, RT activity was decreased in the presence of cell lysate from both types of T cells, however, the lysate from $CD4^+$ T cells impaired the RT activity more strongly than that from $CD4^+8^+$ T cells (Table 1). These results indicate that $CD4^+8^+$ T cells possess a favorable environment for intracellular reverse transcription.

Table 1. Effect of cell lysates on RT activity

RT source	Cell lysates			
	$CD4^+$T cells	$CD4^+8^+$ T cells	No lysates	p value[c]
SIVmac239	332 ± 15[a]	765 ± 158	1665 ± 271	$p < 0.05$
SHIV3rN	802 ± 75	1086 ± 98	9346 ± 1883	$p < 0.05$
M-MLV-RT[b]	17039 ± 1218	53211 ± 1619	100713 ± 13490	$p < 0.01$

Cell lysates were prepared from $CD4^+$ and $CD4^+8^+$ T cells. RT assay was performed in the presence or absence of cell lysates

[a] cpm/10 μg protein

[b] Moloney Murine Leukemia Virus Reverse Transcriptase (Gibco): 8.3 U

[c] $CD4^+$ T cells versus $CD4^+8^+$ T cells

Discussion

We observed in this study that SIV replicated more efficiently in $CD4^+8^+$ T cells than in $CD4^+$ T cells, of which expression levels of receptors and turnover rate were almost the same. We therefore set out to focus at which steps SIV replication was accelerated in $CD4^+8^+$ T cells. We found that reverse transcription initiated more efficiently in $CD4^+8^+$ T cells than in $CD4^+$ T cells. Therefore, we presumed that intracellular environment in $CD4^+8^+$ T cells was optimal for reverse transcription. After the entry of virus, productive HIV-1/SIV infection requires overcoming several cellular blocks in the establishment of provirus and its replication. There have been significant advances in the identification of cellular cofactors that affect events in HIV-1 replication after entry of virus [23]. Kinoshita et al. demonstrated that a nuclear factor of activated T cells (NFAT) overcame a blockade at reverse transcription and permitted active HIV-1 replication [13]. Although the target genes for NFAT that can aid completed reverse transcription are unknown, NFAT appears to be involved in HIV-1 replication at pre- and post integrative steps of the HIV-1 life cycle. Although we have not yet determined whether NFAT expression was more greatly enhanced in $CD4^+8^+$ T cells, it is possible that $CD4^+8^+$ T cells contain either known or unknown factors that permit reverse transcription like NFAT, or fewer cellular factors that inhibit reverse transcription.

Many investigators have provided evidence for the widespread infection of CD8 T cells by HIV-1/SIV both in vitro and in vivo [5, 10]. In most cases, transient co-expression of CD4 during maturation or activation renders them susceptible to HIV-1/SIV infection and destruction [14, 29]. In our case, the efficiency of virus entry into $CD4^+8^+$ T cells was almost the same as into $CD4^+$ T cells. An important issue is whether the expression of CD8 molecules on $CD4^+8^+$ T cells is related to induce a higher permissive state for virus replication. To solve this question, we are currently designing the experiment using CD8 specific RNAi which offers a valuable opportunity to modulate the expression of cellular genes.

We have established $CD4^+8^+$ T cells and $CD4^+$ T cells from rhesus macaque PBMC. $CD4^+8^+$ T cells in PBMC are observed in approximately 3% of human and 5% of rhesus macaques [11, 22]. Several reports have shown that activation of $CD8^+$ T cells from peripheral blood resulted in the de novo expression of CD4 molecule and these peripheral $CD4^+8^+$ T cells were in the activated states [2, 14, 24]. Also, it has been reported that the majority of the intestinal T cells including $CD4^+8^+$ T cells are memory T cells and are in an activated state [12]. Since HIV-1/SIV is assumed to preferentially infect and kill the activated T cells [28], $CD4^+8^+$ T cells in the peripheral blood or the intestine may be readily infected by the virus and produce a large amount of virus. The high level of viral production disseminates infection systemically and provides access to large numbers of target cells for prolonged replication. The function of $CD4^+8^+$ T cell subset in these organs is not fully defined, however, we speculate that infected $CD4^+8^+$ T cells might play an important role for early viral dissemination and

serve as a potent viral reservoir in HIV-1/SIV infection. On the other hand, we observed that the number of viable cells in infected $CD4^+$ T cells were considerably more than that in infected $CD4^+8^+$ T cells, which indicated that the depletion of $CD4^+$ T cells by SIV infection were less. Previous studies have also shown that the depletion of $CD4^+$ T cells in PBMC was gradual in HIV-1/SIV infection [11]. The low level of viral replication could provide a mechanism for cells to escape the host defense surveillance and favor establishment of a persistent infection. Therefore, although there were little differences between $CD4^+$ T cells and $CD4^+8^+$ T cells in the expression level of receptors, both types of CD4 positive cells might play distinct roles in HIV-1/SIV infection.

In the present study, we compared the susceptibility to SIV infection in $CD4^+$ T cells and $CD4^+8^+$ T cells using HVS-transformed T cell lines. Although we have not confirmed our findings by ex vivo analysis using PBMC from rhesus macaques, our model may be helpful in understanding the viral replication and reservoirs in vivo.

Acknowledgments

We thank Dr. M. Yasukawa for generously providing the 488 strain of H. saimiri group C.

References

1. Akahata W, Ido E, Hayami M (2003) Mutational analysis of two zinc finger motifs in the nucleocapsid protein of SIVmac239. J Gen Virol 84: 1641–1648
2. Blue ML, Daley JF, Levine H, Craig KA, Schlossman SF (1986) Biosynthesis and surface expression of T8 by peripheral blood $T4^+$ cells in vitro. J Immunol 137: 1202–1207
3. Calabro ML, Zanotto C, Calderazzo F, Crivellaro C, Mistro AD, Rossi AD, Chieco-Bianchi L (1995) HIV-1 infection of the thymus: evidence for a cytopathic and thymotropic viral variant in vivo. AIDS Res Hum Retrovir 11: 11–19
4. Calabro ML, Zanotto C, Calderazzo F, Crivellaro C, Mistro AD, Rossi AD, Chieco-Bianchi L (1995) HIV-1 infection of the thymus: evidence for a cytopathic and thymotropic viral variant in vivo. AIDS Res Hum Retrovir 11: 11–19
5. Dean GA, Reubel GH, Pedersen NC (1996) Simian immunodeficiency virus infection of $CD8^+$ lymphocytes in vivo. J Virol 70: 5646–5650
6. Deng H, Liu R, Wllmeier W, Choe S, Unutmaz D, Burkhart M, Di Marzio P, Marmon S, Sutton RE, Hill CM, Davis CB, Peiper SC, Schall TJ, Littman DR, Landau NR (1996) Identification of a major co-receptor for primary isolates of HIV-1. Nature 381: 667–678
7. Dusserre N, Dezutter-Dambuyant C, Mallet F, Delorme P, Philit F, Ebersold A, Desgranges C, Thivolet J, Schmitt D (1992) In vitro HIV-1 entry and replication in Langerhans cells may clarify the HIV-1 genome detection by PCR in epidermis of seropositive patients. J Invest Dermatol 99: 89S–102S
8. Feng Y, Broder CC, Kennedy PE, Berger EA (1996) HIV-1 entry cofactor: functional cDNA cloning of a seven-transmembrane, G protein-coupled receptor. Science 272: 872–877
9. Hirsch VM, Sharkey ME, Brown CR, Brichacek B, Goldstein S, Wakefield J, Byrum R, Elkins WR, Hahn BH, Lifson JD, Stevenson M (1998) Vpx is required for dissemination

and pathogenesis of SIVsm Pbj: Evidence of macrophage-dependent viral amplification. Nat Med 4: 1401–1408
10. Imlach S, McBreen S, Shirafuji T, Leen C, Bell JE, Simmonds P (2001) Activated peripheral CD8 lymphocytes express CD4 in vivo and are targets for infection by human immunodeficiency virus type 1. J Virol 75: 11555–11564
11. Jason J, Inge KL (2001) Modulation of CD8 and CD3 by HIV or HIV antigens. Scand J Immunol 53: 259–267
12. Kahn JO, Walker BD (1998) Acute human immunodeficiency virus type 1 infection. N Engl J Med 339: 33–39
13. Kinoshita S, Chen BK, Kaneshima H, Nolan GP (1998) Host control of HIV-1 parasitism in T cells by the nuclear factor of activated T cells. Cell 95: 595–604
14. Kitchen SG, JaForge S, Patel VP, Kitchen CM, Miceli MC, Zack JA (2002) Activation of CD8 T cells induces expression of CD4, which functions as a chemotactic receptor. Blood 99: 207–212
15. Kitchen SG, Jones NR, LaForge S, Whitmire JK, Vu BA, Galic Z, Brooks DG, Brown SJ, Kitchen CMR, Zack JA (2004) CD4 on $CD8^+$ T cells directly enhances effector function and is a target for HIV infection. Proc Natl Acad Sci USA 101: 8727–8732
16. Kumar A, Stipp HL, Sheffer D, Narayan O (1999) Use of herpesvirus saimiri-immortalized macaque $CD4^+$ T cell clones as stimulators and targets for assessment of CTL responses in macaque/AIDS models. J Immunol Methods 230: 47–58
17. Levy JA (1993) Pathogenesis of human immunodeficiency virus infection. Microbiol Rev 57: 183–289
18. Marx PA, Spira AI, Gettie A, Dailey PJ, Veazey RS, Lackner AA, Mahoney CJ, Miller CJ, Claypool LE, Ho DD, Alexander NJ (1996) Progesterone implants enhance SIV vaginal transmission and early virus load. Nat Med 2: 1084–1089
19. Mattapallil JJ, Smit-McBride Z, McChesney M, Dandekar S (1998) Intestinal intraepithelial lymphocytes are primed for gamma interferon and MIP-1β expression and display antiviral cytotoxic activity despite severe $CD4^+$ T-cell depletion in primary simian immunodeficiency virus infection. J Virol 72: 6421–6429
20. Rowland-Jones S (1999) HIV infection: where have all the T cells gone? Lancet 354: 5–7
21. Smit-McBride Z, Mattapallil JJ, McChesney M, Ferrick D, Dandekar S (1998) Gastrointestinal T lymphocytes retain high potential for cytokine responses by have severe $CD4^+$ T-cell depletion at all stages of simian immunodeficiency virus infection compared to peripheral lymphocytes. J Virol 72: 6646–6656
22. Stanley SK, McCune JM, Kaneshima H, Justement JS, Sullivan M, Boone E, Baseler M, Adelsberger J, Bonyhadi M, Orenstien J, Fox CH, Fauci AS (1993) Human immunodeficiency virus infection of the human thymus and disruption of the thymic microenvironment in the SCID-hu mouse. J Exp Med 178: 1151–1163
23. Stevenson M (2003) HIV-1 pathogenesis. Nat Med 9: 853–860
24. Sullivan YB, Landay AL, Zack JA, Kitchen SG, Al-Harthi L (2001) Upregulation of CD4 and $CD8^+$ T cells: CD4dimCD8bright T cells constitute an activated phenotype of $CD8^+$ T cells. Immunology 103: 270–280
25. Takahashi M, Osono E, Nakagawa Y, Wang J, Berzofsky JA, Margulies DH, Takahashi H (2002) Rapid induction of apoptosis in $CD8^+$ HIV-1 envelope-specific murine CTLs by short exposure to antigenic peptide. J Immunol 169: 6588–6593
26. Willey RL, Smith DH, Lasky LA, Theodore TS, Earl PL, Moss B, Capon DJ, Martin MA (1988) In vitro mutagenesis identifies a region within the envelope gene of the human immunodeficiency virus that is critical for infectivity. J Virol 62: 139–147

27. Yasukawa M, Inoue Y, Kimura U, Fujita S (1995) Immortalization of human T cells expressing T-cell receptor gamma delta by herpesvirus saimiri. J Virol 69: 8114–8117
28. Zhang ZQ, Schuler T, Zupancic M, Wietgrefe S, Sraskus KA, Reimann KA, Reinhart TA, Rogan M, Cavert W, Miller CJ, Veazey RS, Notermans D, Little S, Danner SA, Richman DD, Havlir D, Wong J, Jordan HL, Schacker TW, Racz P, Tenner-Racz K, Letvin NL, Wolinsky S, Haase AT (1999) Sexual transmission and propagation of SIV and HIV in resting and activated $CD4^+$ T cells. Science 286: 1353–1357
29. Zloza A, Sullivan YB, Connick E, Landay AL, Al-Harthi L (2003) $CD8^+$ T cells that express CD4 on their surface ($CD4^{dim}CD8^{bright}$ T cells) recognize an antigen-specific target, are detected in vivo, and can be productively infected by T-tropic HIV. Blood 102: 2156–2164

Author's address: Hidemi Takahashi, M.D., PhD., Department of Microbiology and Immunology, Nippon Medical School, 1-1-5, Sendagi, Bunkyo-ku, Tokyo 113-8602, Japan; e-mail: htkuhkai@nms.ac.jp

Tissue Antigens ISSN 0001-2815

Analysis of evolutionary conservation in CD1d molecules among primates

N. Saito[1,2], M. Takahashi[1,3], W. Akahata[2], E. Ido[2], C. Hidaka[3], K. Ibuki[2], T. Miura[2], M. Hayami[2] & H. Takahashi[1,3]

1 Laboratory of Virus Control, Institute for Virus Research, Kyoto University, 53 Shogoin-Kawahara-cho, Kyoto 606-8507, Japan
2 Laboratory of Primate Model, Institute for Virus Research, Kyoto University, 53 Shogoin-Kawahara-cho, Kyoto 606-8507, Japan
3 Department of Microbiology and Immunology, Nippon Medical School, 1-1-5, Sendagi, Bunkyo-ku, Tokyo 113-8602, Japan

Key words
African green monkey; CD1d; chimpanzee; HIV-1/ SIV; NKT; primate; rhesus monkey; susceptibility

Correspondence
Hidemi Takahashi, MD, PhD
Department of Microbiology and Immunology
Nippon Medical School
1-1-5, Sendagi, Bunkyo-ku
Tokyo 113-8602, Japan
Tel: 81 3 3822 2131x5381
Fax: 81 3 3316 1904
e-mail: htkuhkai@nms.ac.jp

Received 15 June 2005; revised 15 August 2005; re-revised 28 August 2005; accepted 2 September 2005

doi: 10.1111/j.1399-0039.2005.00504.x

Abstract

The hereditary conservation in the genetically encoded *CD1D* sequences of various primates was analyzed. Genomic *CD1D* sequences of 17 rhesus macaques with distinct origins, eight Indian and nine Chinese, were examined and differences of only one or two nucleotides were detected and the consensus sequence of rhesus *CD1D* was determined. *CD1D* consensus sequences of three African green monkeys (AGMs) and the rhesus monkeys were then compared to study the evolutionary differences among interspecies. The *CD1D* consensus sequence determined from AGMs apparently differed by seven nucleotides from the rhesus consensus sequence, and nucleotide difference induced only three amino acid changes within Exon3, corresponding to the α_2 domain of CD1d having a hydrophobic ligand-binding pocket. Such changes in the α_2 domain may alter the characteristics of the SIV-derived glycolipid/lipid antigens presented by each CD1d molecule to innate natural killer T cells. In addition, the *CD1D* genomic sequences of three chimpanzees (chimps) were determined. To our surprise, although Exon2 and Exon3 reflecting antigen-binding α_1 and α_2 domains in chimps' *CD1D* were identical to that in humans except one amino acid, three amino acids within Exon4, reflecting α_3 domain, were distinct from humans, and one of them was identical to those in rhesus and AGM *CD1D*. On the basis of the findings, the evolutionary relationship of the CD1d molecules among the various primates and their HIV-1/SIV susceptibility will be discussed.

Introduction

Unlike B lymphocytes bearing immunoglobulin receptors that can bind directly onto various free antigens, T lymphocytes can recognize foreign antigens as their processed fragments in conjunction with antigen-presenting molecules on the surface of antigen-presenting cells (APCs) (1). Such antigen-presenting molecules are usually classified into three groups: class I major histocompatibility complex (MHC), class II MHC, and CD1. The first two MHC molecules can present processed peptide antigens, whereas the last CD1 can present glycolipid/lipid antigens derived from various pathogens (2). In general, endogenously synthesized foreign antigens such as viral proteins are degraded into peptide fragments composed of eight to 10 amino acids in the cytosol through an ATP-dependent proteolytic system, trapped into the class I MHC groove and presented to specific $CD8^+$ T lymphocytes (3). In contrast, free soluble and particulate peptide antigens from various pathogens are captured exogenously by APCs such as immature dendritic cells (iDCs), transported to acidic endosomal compartment, where the captured antigens are further degraded to fit into the channel of class II MHC, and the peptide-loaded class II MHC molecules are exported to the cell surface for the stimulation of antigen-specific $CD4^+$ T lymphocytes (4).

As for CD1 antigen presentation, there have been four distinct types of CD1 molecules (CD1a, b, c, and d) identified on the surface of human APCs, and two subclasses

of CD1d are found in mice to present glycolipid/lipid but not conventional processed peptide antigens (5, 6). On the basis of sequence homologies, these CD1 molecules can be classified into two types: CD1a, b, and c as group 1 and CD1d as group 2 (7). These CD1 molecules present unique glycolipid/lipid antigens with amphipathic structure whose hydrophobic lipid tails are bound to deep cavity in the CD1s and present lipid–sugar complex to T cells expressing αβ T-cell receptors (TCRs). For example, CD1a presents dideoxymycobactin (DDM) (8), CD1b lipoarabinomannan (LAM) (9), glucose monomycolate (GMM) (10), and mycolic acid (11); CD1c mannosyl phosphoisoprenoid (12) and CD1d glycosyl-phosphatidyl inositol (GPI) (13); or α-galactosyl ceramide (αGalCer) (14). Such glycolipid/lipid antigens presented by the group 1 CD1 molecule (CD1a, b, and c) on DCs stimulate conventional αβ TCR-bearing T cells expressing either $CD8^+$ T cells or $CD4^-CD8^-$ T cells, whereas antigens presented by group 2 CD1 (CD1d) on DCs, as well as various types of mononuclear cells, such as T cells, B cells, and monocytes, activate natural killer T (NKT) cells. NKT cells are a subset of T cells expressing not only NK receptor but also invariant αβ TCRs such as Vα24 TCR in humans (15) and Vα14 in mice (16) for the recognition of glycolipid/lipid antigens like αGalCer presented by the CD1d.

The structures of these CD1 molecules are similar to those of class I MHCs bearing noncovalently bound β_2 microglobulin; however, the CD1s show limited polymorphism and do not map to the MHC genes (17). Moreover, although class I and II MHC molecules are extremely diverse among species with self-restricted elements that can present processed antigens only to the same MHC-bearing cells, the CD1-encoding genes are highly conserved, and their structures are shared among species (18), indicating the importance of CD1-restricted effectors for maintaining species evolution, and mutation or inactivation of the CD1s might deprive the species continuity. Furthermore, the fact that mice and rats have only CD1d among other classical CD1s in a highly conserved manner (19) reveals that the preservation of CD1d molecules together with NKT cells as their evolutionarily selected partners seems to be critical for such rodents to evolve.

In the present study, we focused on analyzing the hereditary conservation in the genetically encoding *CD1D* sequences of various primates. To date, human and rodent *CD1D* sequences (20–22) and some portion of genomic DNA of rhesus macaque have been reported (23). Therefore, we first confirmed whether the genomic DNA sequence of *CD1D* was identical to the cDNA encoding *CD1D* message by establishing iDCs from peripheral blood mononuclear cells (PBMCs) of rhesus macaques to determine the *CD1D* consensus sequence. We then compared the *CD1D* sequences of African green monkeys (AGMs) and rhesus monkeys to see the evolutionary difference in the CD1d molecules among interspecies. Finally, we determined for the first time the genomic sequences of *CD1D* in chimpanzees (chimps) for comparison. On the basis of the findings obtained here, the evolutionary relationship in the CD1d molecules among various primates and their HIV-1/SIV susceptibility as models for HIV-1 infection will be discussed.

Materials and methods

Animals

Seventeen rhesus macaques (*Macaca mulatta*), nine Chinese originated and eight Indian originated, and three AGMs (*Cercopithecus aetiops grivet*) were used in this experiment. All monkeys used in this study were housed in accordance with regulations approved by the Institutional Animal Care and Use Committee of the Institute for Virus Research, Kyoto University. Three blood samples of chimps (*Pan troglodytes*) were kindly obtained from Dr S. Singh (Cornell University).

Induction of iDCs from PBMCs

PBMCs of rhesus macaques were isolated from heparinized blood by density gradient centrifugation using Lymphocyte Separation Solution (Nakarai Tesque, Kyoto, Japan) and cultured in monocyte-separating plates (MSP-P) (JIMRO, Gunma, Japan) at 1×10^7 cells in 2.5 ml of Dulbecco's modified Eagle medium (DMEM) (Gibco-BRL, Grand Island, NY), supplemented with 10% fetal calf serum (FCS) for 1–2 h in a 5% CO_2 incubator at 37°C as described recently (24). After incubation, the non-adherent cells were removed, and the adherent monocytes were further cultured in 2.5 ml DMEM supplemented with 10% FCS, 200 ng/ml recombinant human granulocyte macrophage-colony-stimulating factor (rhGM-CSF) (R&D system, Minneapolis, MN), and 50 ng/ml recombinant human interleukin-4 (rhIL-4) (R&D system) for an additional 6–8 days to generate the CD1-expressing monocyte-derived iDCs as described previously (25).

RNA extraction from rhesus iDCs and cDNA synthesis

RNAs were extracted from the established monocyte-derived iDCs using total RNA isolation reagent for the liquid samples (TRIZOL; Gibco-BRL). Then poly-A-tailed mRNAs were collected from the extracted total RNA and changed into cDNA with a first-strand cDNA Synthesis Kit (Invitrogen, Carlsbad, CA).

Cloning of *CD1D*-encoding genes

Preparation of PCR product

In order to proceed with the cloning of rhesus *CD1D* genes, the cDNA obtained was added to a mixture

containing 10 mM Tris–HCl (pH 8.3), 50 mM KCl, 2.5 mM $MgCl_2$, 200 μM of each dNTPs, 0.2 μM of each primer, and 2.5 units of AmpliTaq DNA polymerase (Roche Diagnostics GmbH, Mannheim, Germany). The amplification of cDNA fragments was performed for 35 cycles consisting of the following three steps: denaturation at 94°C for 60 s (5 min for the first cycle), annealing at 55°C for 60 s, and elongation at 72°C for 90 s (5 min for the last cycle). The primers shown below were estimated on the basis of human *CD1D* sequences (26): CD1d (forward) (5′-TTCACA GGACGCCCTGATAGGAACTTTGCCTCTTAAACC-GGGAGGTAAAGCCCAC-3′) and CD1d (reverse) (5′-TCAGGACGCCCTGATAGGAACTTTGCCTCTTAA-ACCGGGAGGTAAAGCCCAC-3′).

Subcloning of PCR product

The PCR products were then run in a 1.5% agarose gel supplemented with ethidium bromide. The specified bands were excised and purified using a QIAquick Gel Extraction Kit (Qiagen, Valencia, CA). Purified cDNAs were ligated into a pCR2.1-TOPO TA cloning vector (Invitrogen) and inserted into their competent cells (*Escherichia coli*-derived DH5α; Invitrogen). After 24 h incubation, white colonies were picked for sequencing experiments. Twelve white colonies from LB plate were picked up and the sequence analysis was performed on four clones. Three sequencing experiments were carried out to account for false positive.

Sequence analysis of cloned cDNA

Sequence analysis was performed using a DNA sequencing Kit (Big Dye Terminator Cycle Sequencing Ready Reaction; Applied Biosystems, Foster city, CA). The amplification of cDNA fragments was performed for 25 cycles, consisting of denaturation at 96°C for 10 s, annealing at 50°C for 5 s, and elongation at 60°C for 4 min. Sequences of amplified DNA fragments were determined with an ABI PRISM 3100 Genetic Analyzer (Applied Biosystems). M13 primers were used for sequencing analysis: M13 (forward) (5′-GTAAAACGACGGCCAG-3′) and M13 (reverse) (5′-CAGGAAACAGCTATGAC-3′).

Direct sequencing of *CD1D* from genomic DNA

Genomic DNA was extracted from PBMCs of various primates with QIAamp DNA Mini Kit (Qiagen GmbH, Hilden, Germany). Then the genomic DNA was subjected to the PCR. The following primers were prepared on the basis of human genomic *CD1D* sequence (26):

Exon1 E1F (5′-AGAAGAGTGCGCAGGTCAGAGG GCGGCCGC-3′)
E1R (5′-CGCCAGTGCGTCCCGGGTCTCAC CAGT CCC-3′)
Exon2 E2F (5′-ATGCTGGCTGCTCTCCCGGCC ACTTGCTAC-3′)
E2R (5′-TCTGTGGCCATTCTCTCCCCTT GGGTAC CG-3′)
Exon3 E3F (5′-TCTCTTTCATCTCTCCCAGTCT TTTAAAC-3′)
E3R (5′-GGAAAAGCCCGTTTGGAGCCC TGAAG TGGA-3′)
Exon4 E4F (5′-GGAGCCTCTAATGCAGAGTTT TCACTTTAA-3′)
E4R (5′-CACCCCAGTGCCTCCCTCTAT GCCTGA GGA-3′)
Exon5–6 E5F (5′-ATTGGGGTTTTAAGTGGAG GAGGAAATAAG-3′)
E5R (5′-TTTCAAGGTATCTCTCCTATCT TCAATT CC-3′)

The amplification of DNA fragments was performed for 35 cycles, consisting of denaturation at 94°C for 30 s (5 min for the first cycle), annealing at 60°C for 30 s, and elongation at 72°C for 45 s (5 min for the last cycle) and confirmed with agarose gel electrophoresis. The DNA fragments were purified and then analyzed with an ABI PRISM 3100 Genetic Analyzer. In the case of the thin fragments, they were ligated into the TA cloning site of pCR 2.1-TOPO Vector (TOPO TA Cloning; Invitrogen) and inserted into their competent cells (*Escherichia coli*-derived DH5α; Gibco-BRL). The plasmid was prepared by the alkaline lysis method (27), and the purified plasmid was used for sequence analysis.

GenBank accession

Each determined sequence of the *CD1D* was submitted to public database and obtained the GenBank accession numbers as follows:

C-1 to C-7 and C-9 are corresponding to the numbers of AB222829 to AB222836, respectively, and C-8 is to AB232047. I-1 to I-8 are corresponding to the numbers of AB222837 to AB222844, respectively. Three AGMs are corresponding to the numbers of AB222994 to AB222996 and three chimps are to AB222997, AB222998, and AB223044, respectively.

Results

Establishment of iDCs from PBMCs of a rhesus macaques and the cloning and sequencing of their CD1d molecules

Because CD1d molecules are generally expressed on DCs or iDCs, we first established the iDCs from freshly isolated PBMCs of a rhesus macaque named MM257 by culturing them with GM-CSF and rhIL-4, as previously indicated. Then, total RNA was extracted from those iDCs, and the cDNA of *CD1D* was cloned from the mRNA using reverse

transcriptase. As shown in Figure 1, the size of rhesus *CD1D* cDNA was 1014 bp, similar to that of human *CD1D* that has been reported previously (26). The cloned cDNA was inserted into competent cells for sequence analysis using a TA-cloning vector. Consequently, we obtained four clones, and their sequences were analyzed using a Genetic Sequencing Analyzer. As represented in Figure 2, we managed to determine the *CD1D* sequence of rhesus MM257. However, since only human GM-CSF and IL-4 were available to induce DCs from various primates, we have experienced serious difficulty in establishing primates' DCs from PBMCs. We thus attempted to confirm whether the genomic DNA sequence for *CD1D* was similar to the *CD1D* message encoded in the cDNA to determine the *CD1D* consensus sequence and found that both sequences were identical in the rhesus MM257 (data not shown). Therefore, we examined the genomic DNA instead of the mRNA-derived cDNA for further analysis.

Comparison of *CD1D* sequences among rhesus macaques with distinct origins

In contrast to class I and class II MHC molecules composed of distinct sequences of amino acids in each individual even among the same species, CD1 molecules consist of species-specific and highly conserved sequences (22). Therefore, we speculated that the *CD1D* sequence of MM257 would probably be the same as other rhesus macaques. We examined the genomic *CD1D* sequences of 16 additional rhesus macaques. The former eight macaques originated from China including MM257 and the latter eight were from India. As expected, in comparison with the whole *CD1D* sequences of MM257, only one or two nucleotide differences could be found among other samples, and the consensus sequence of the rhesus *CD1D* was determined from the results (Table 1). Since these nucleotide changes affected only one amino acid alteration

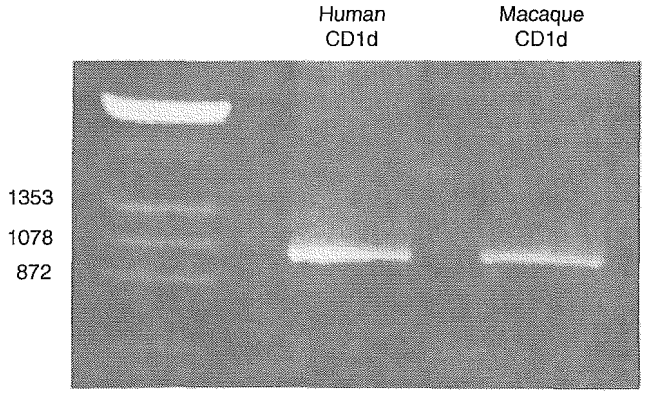

Figure 1 Amplification of the rhesus macaque *CD1D* cDNA from monocyte-derived immature dendritic cells. The size of specific band (bp) obtained by RT-PCR was similar to that of human CD1d.

at position 896, Leu for MM257 and His for other monkeys in Exon5, such changes do not have an influence on antigen presentation by CD1d molecules (28).

Comparison of *CD1D* sequences between rhesus macaques and AGMs

Because the susceptibility to SIV is totally different between rhesus macaques and AGMs in that the rhesus macaques will develop immune-deficient states with marked decrease in CD4, whereas the latter AGMs will not, although AGMs have been thought as natural hosts of SIV (29); we examined whether the *CD1D* sequences were genetically conserved between those species. As shown in Table 2, the consensus *CD1D* sequence determined from the AGMs differed by seven nucleotides from the rhesus consensus sequence. Nevertheless, these nucleotide differences resulted in three amino acid changes within Exon3, corresponding to the α_2 domain of CD1d, having a hydrophobic ligand-binding pocket (28).

Comparison of the consensus *CD1D* sequences of rhesus macaques and AGMs with those of chimps and humans

These rhesus macaques and AGMs are not susceptible to HIV-1, but both chimps and humans are susceptible to HIV-1, but not to SIV (30). We thus conducted direct sequencing for *CD1D* using PBMCs obtained from three chimps (kindly provided by Dr S. Singh, Cornell University) to determine the consensus *CD1D* sequence of chimps. Nucleotide sequences (Figure 3A) and amino acid alignments (Figure 3B) among humans, chimps, rhesus macaques, and AGMs are summarized. Unexpectedly, both Exon2 and Exon3, reflecting the antigen-binding sites of the α_1 and α_2 domains, were identical except for one amino acid, Glu(E), at position 182 between chimps and humans. However, three amino acids, Asp (D), Ala (A), and Ile (I), at positions 229, 252, and 274 within Exon4, reflecting α_3 domain, were distinct from humans, and one of them was identical to those in rhesus and AGM *CD1D*. Moreover, on the basis of recent reports on the precise structural analysis of CD1d molecules for antigen presentation to NKT cells (31–34), we boxed the amino acid sequences crucial for antigen presentation and highlighted the amino acids critical for human NKT-cell activation among them (Figure 3B).

Discussion

In the present study, we first determined the *CD1D* sequence of a rhesus macaque, named MM257, from mRNA-derived cDNA clones and confirmed the consistency of the sequence with genomic DNA obtained from MM257 PBMC to decide the consensus sequence. We then

```
        10         20         30         40         50         60         70         80         90         100        110        120
ATGGGGTGCCTGCTGTTTCTGCTGCTCTGGGCGCTCCTCCAGGCTTGGGGAAGCGCTGAAGTCCCGCAAAGGCTTTTCCCCCTCCGCTGCCTCCAAATCTCGTCCTTCGCCAATAGCAAC
M  G  C  L  L  F  L  L  L  W  A  L  L  Q  A  W  G  S  A  E  V  P  Q  R  L  F  P  L  R  C  L  Q  I  S  S  F  A  N  S  N

        130        140        150        160        170        180        190        200        210        220        230        240
TGGACGCGCACCGATGGTTTGGCGTGGCTGGGGGAGCTGCAGACGCACAGCTGGAGCAACGACTCCGACACCATCCGCTCTCTGAAGCCGTGGTCCCAGGGCACGTTCAGCGACCAGCAG
W  T  R  T  D  G  L  A  W  L  G  E  L  Q  T  H  S  W  S  N  D  S  D  T  I  R  S  L  K  P  W  S  Q  G  T  F  S  D  Q  Q

        250        260        270        280        290        300        310        320        330        340        350        360
TGGGAGGCGCTGCAGCGTGTATTTCGGGTTTATCGAAGCAGCTTCACCAGGGACGTGAAGGAATTCGCCAAAATGCTGCGCTTAGCCTATCCCATGGAGCTCCAGGTGTCTGCTGGCTGT
W  E  A  L  Q  R  V  F  R  V  Y  R  S  S  F  T  R  D  V  K  E  F  A  K  M  L  R  L  A  Y  P  M  E  L  Q  V  S  A  G  C

        370        380        390        400        410        420        430        440        450        460        470        480
GAGGTGCACCCTGGAAACGCCTCACATAACTTCTTCCATGTAGCGTTTCAAGGAAGTGATATCCTGAGTTTCCAAGGAACTTCTTGGGAACCAGCCCAAGAGGCCCCACTTTGGGTAAAC
E  V  H  P  G  N  A  S  H  N  F  F  H  V  A  F  Q  G  S  D  I  L  S  F  Q  G  T  S  W  E  P  A  Q  E  A  P  L  W  V  N

        490        500        510        520        530        540        550        560        570        580        590        600
TTGGCCATCCAAGTGCTCAACCAGGACAACTGGACGAAGGAAACAGTGCAGTGGCTCCTTAATGACACCTGCCCCCAATTTGTCAGTGGCCTCCTTGAGTCAGGGAAGTCGGAACTGGAG
L  A  I  Q  V  L  N  Q  D  N  W  T  K  E  T  V  Q  W  L  L  N  D  T  C  P  Q  F  V  S  G  L  L  E  S  G  K  S  E  L  E

        610        620        630        640        650        660        670        680        690        700        710        720
AAGCAAGTGAAGCCCAAGGCCTGGCTGTCCCGTGGCCCCAGTCCTGGCCCTGGCCGTCTGCAGCTTGTGTGCCATGTCTCAGGATTCTACCCAAAGCCCGTGTGGGTGAAGTGGATGCGG
K  Q  V  K  P  K  A  W  L  S  R  G  P  S  P  G  P  G  R  L  Q  L  V  C  H  V  S  G  F  Y  P  K  P  V  W  V  K  W  M  R

        730        740        750        760        770        780        790        800        810        820        830        840
GGTGAGCAGGAGCAGCAGGGCACTCAGCGAGGGGACATCCTGCCCAATGCTGACGAGACATGGTATCTCCGAGCAACCCTGGAGGTGGCCGCTGGGGAGGCAGCTGGCCTGTCCTGTCGG
G  E  Q  E  Q  Q  G  T  Q  R  G  D  I  L  P  N  A  D  E  T  W  Y  L  R  A  T  L  E  V  A  A  G  E  A  A  G  L  S  C  R

        850        860        870        880        890        900        910        920        930        940        950        960
GTGAAGCACAGCAGTCTAGAGGGCCAGGACATCGTCCTCTACTGGGGTGGGAGCCTCACCTCCGTGGGCTTGATCGCCTTGGCAGTCCTGGCATGCTTGCTGTTCCTCCTTGCACTCATT
V  K  H  S  S  L  E  G  Q  D  I  V  L  Y  W  G  G  S  L  T  S  V  G  L  I  A  L  A  V  L  A  C  L  L  F  L  L  A  L  I

        970        980        990        1000       1010       1020
GTAGGCTTTACCTTCCGGTTTAAGAGGCAAACTTCCTATCAGGGCATCCTGTGA
V  G  F  T  F  R  F  K  R  Q  T  S  Y  Q  G  I  L  *
```

Figure 2 Nucleotide and amino acid sequences of the CD1d molecule for rhesus MM257. PCR product obtained from cDNA of MM257 was inserted into a TA cloning vector and sequenced using a DNA sequencer. Analysis of the sequences was performed by GENETYX-MAC software.

Table 1 Comparison of the *CD1D* nucleotide sequences in rhesus macaques of distinct origins

Chinese

Position (bp)	Genomic region	C-1[a]	C-2	C-3	C-4	C-5	C-6	C-7	C-8	C-9	Consensus
96	Exon2	A		G				A/G		A/G	A
199		T	C								T
450	Exon3	A		A/G	A/G	A/G	G	A/G	A/G	G	A/G
510		C			G					C/G	C
555		C			C/T					C/T	C
896	Exon5	T	A	A	A	A	A	A	A	A	A

Indian

Position (bp)	Genomic region	I-1	I-2	I-3	I-4	I-5	I-6	I-7	I-8	Consensus
96	Exon2	A				G	A/G	A/G	G	A
199		T	A/T		C/T					T
331	Exon3	C		C/T		C/T	C/T		T	C
443		C	A/C		A/C					C
450		A/G		G	G		G		G	A/G
510		C			C/G		A/G	C/G		C
555		C			C/T		C/T	C/T		C
659	Exon4	T			G					T
838		C			C/T		C/T	C/T		C

Genomic *CD1D* sequences of 17 rhesus macaques, nine Chinese (C-1 to C-9), and eight Indian (I-1 to I-8) origins were examined, and the consensus sequence of the *CD1D* for rhesus macaques was determined.

[a] C-1 corresponds to MM257 in the text.

Table 2 Comparison of the consensus *CD1D* sequences between rhesus macaques and African green monkeys (AGMs)

		Nucleotide		Amino acid	
Position (bp)	Genomic region	AGM consensus	Macaque consensus	AGM consensus	Macaque consensus
93	Exon2	T	C	L	L
96		G	A	Q	Q
210		T	G	P	P
351	Exon3	C	T	S	S
417		A	T	**R**	**S**
510		G	C	**K**	**N**
518		G	A	**R**	**K**

Consensus sequence of the *CD1D* for AGM was determined from three monkeys. Distinct positions for each specific nucleotide and amino acid were shown. Although the consensus *CD1D* sequence of AGMs differed by seven nucleotides from the rhesus consensus sequence, these nucleotide differences induced only three amino acid changes within Exon3 (indicated as bold).

examined the genomic DNA of another 16 macaques with distinct origins and found that the *CD1D* sequence of all the monkeys tested was identical except one amino acid in Exon5. Thus, genetic structure of species-specific CD1d molecules was far more tightly conserved than that expected among the rhesus macaques and would not be affected by long-term environmental stimulation. Also, the results suggest that the mutation of the *CD1D* genes might ruin the species and indicate the importance of the CD1d-restricted NKT-related immunity for species survival. Indeed, we have recently found that the syngeneic thymoma cells were deleted by NKT-like cells when they expressed unfavorable encoding genes such as alpha-fetoprotein (35) and that dysfunction of NKT cells causes autoimmune disorders (36) or deficiencies of CD1d seems to be associated with the impairment of various infectious diseases (37) that might correlate with the disappearance of the primates bearing mutated *CD1D*.

We next examined whether the *CD1D* sequences were genetically conserved between the two distinct types of monkeys, rhesus macaques and AGMs, and found that the *CD1D* consensus sequence determined from the AGMs differed by seven nucleotides from the consensus sequence of rhesus macaques, and those nucleotide differences generated three amino acids changes within Exon3. Because Exon3 corresponds to the α_2 domain of the CD1d molecules having a hydrophobic ligand-binding pocket critical for antigen presentation (28), these changes of the amino acids may alter the capacity of the presented glycolipid/lipid antigens to effector NKT cells. In the case of SIV infection, such changes in the α_2 domain may affect the characteristics of the SIV-derived glycolipid/lipid antigens presented by the CD1d and may induce functional differences of the activated NKT cells that may result in the distinct susceptibility of the monkeys to SIV. If the different susceptibilities to SIV (38) correlate with the fact that AGMs are the coexisting natural hosts of SIV and rhesus macaques are the victims, NKT-associated innate immunity may have some relation to those opposite outcomes. Also, the finding that the amino acid sequences of Exon2 and Exon4 corresponding to α_1 and α_3 domains of the CD1d, respectively, were totally identical between the rhesus and AGMs indicates that the domains would be conserved among monkeys, and changes of the amino acid sequences at the sites would destroy the species continuation.

It is widely known that genomic sequences between humans and chimps are highly conserved, and both are susceptible to HIV-1 but very weakly to SIV as reported previously that SIVcpz has been isolated from chimpanzee (39). Thus, we examined the *CD1D* sequence of chimps and determined their consensus sequence for the first time. Interestingly, both α_1 and α_2 domains of the CD1d of chimps were totally identical to humans except for one amino acid at the end of the Exon3; however, three amino acids in Exon4 were distinct from humans, and one of them was the same as identified in the α_3 domain of rhesus macaques and AGMs. In comparison with class I MHC molecules, such α_3 domain of CD1 has been reported to be firmly preserved among each species (20). Moreover, as shown in the Figure 3B, all the crucial amino acids for lipid/glycolipid antigen presentation were strictly conserved among the primates tested, and thus the presented antigens by the α_1 and α_2 domains of CD1d molecule must be the similar among those primates. These results suggest that NKT response to HIV or SIV may not be determined by the antigens presented by the species-specific CD1d molecules, but rather by the structural difference in the CD1d itself or antigen/CD1d complex. Indeed, as shown in Figure 3B, highlighted amino acids at positions Asp(D)151 and Thr(T)154, critical for human NKT-cell activation to the known glycolipid antigens αGalCer (34), were associated with Lys(K)152 and Arg(R)155 in the α_2 domain of the AGM, human, and chimps' CD1d, while they were linked with Asn(N)152 and Lys(K)155 of macaque CD1d, suggesting that distinct susceptibility to SIV may correlate with the CD1d structure and with the activated status of NKT cells because only rhesus macaques fall into immune-deficient state via SIV infection among them.

Taken together, the findings shown in the present study reveal that the α_1 and α_2 domains of the CD1d molecules may present retroviral glycolipid/lipid antigens to the species-specific NKT cells, which may be associated with the type of infectious viruses as well as the susceptibility to them and suggest the evolutionary relationship between the species-specific CD1d molecules and retrovirus infection through the activation of innate effector NKT cells.

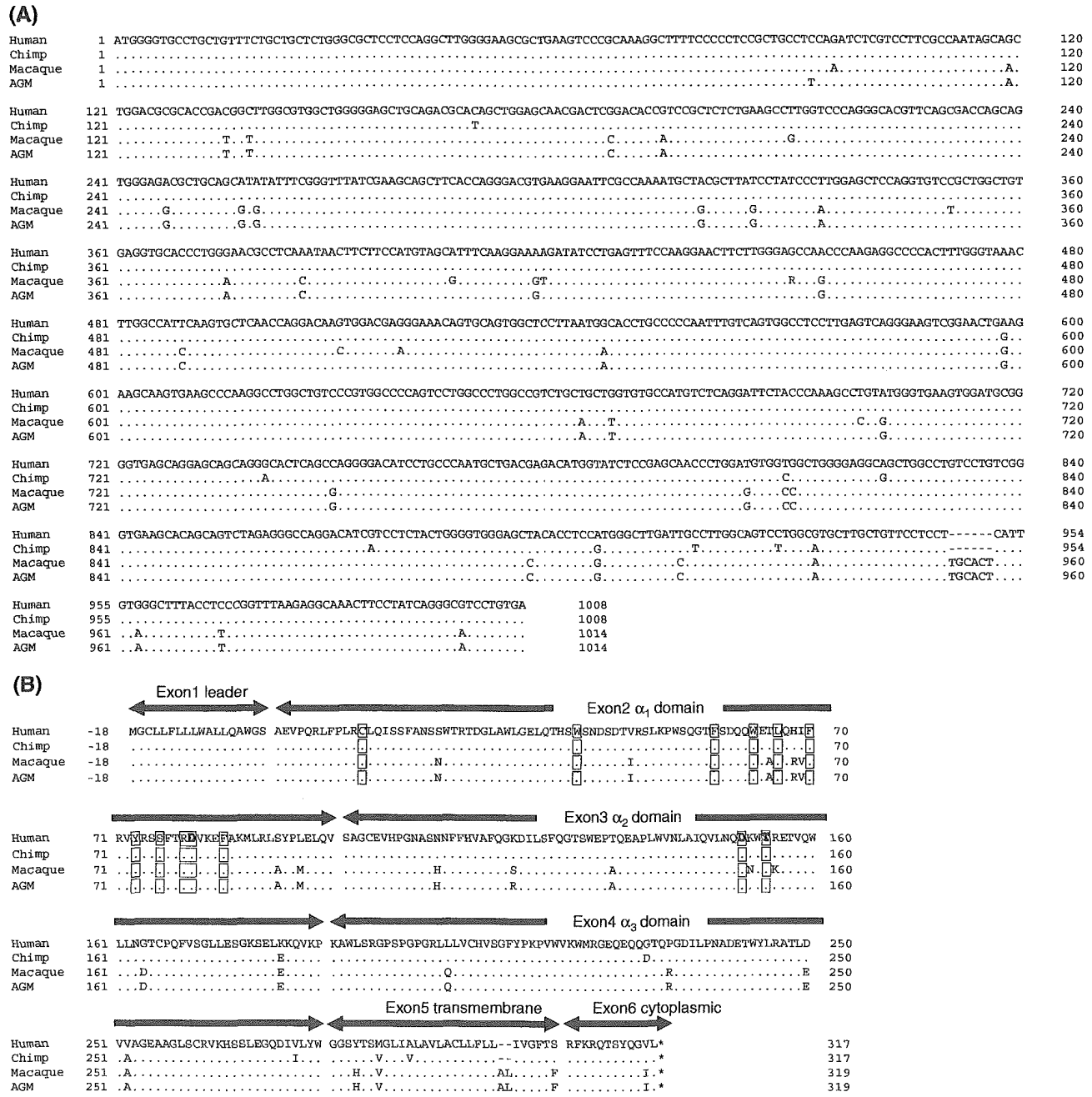

Figures 3 Comparison of consensus *CD1D* sequences between chimpanzees (chimps) and monkeys on the basis of human consensus sequence. (A) Nucleotides alignment of CD1d molecules for each subject. The first line stands for the known human *CD1D*, the second line for the determined chimps' *CD1D*, third line for the rhesus macaques, and the last line for the African green monkeys (AGMs). When the nucleotide was the same with humans, the positions were indicated with dot. (B) Amino acid alignment of CD1d molecules for each subject. Antigen-binding sites, Exon2 and Exon3, were indicated with arrows. Also, the amino acid sequences crucial for antigen presentation were boxed, and those critical for human natural killer T-cell activation among them were highlighted.

Acknowledgments

This work was supported in part by grants from the Ministry of Education, Science, Sport, and Culture, from the Ministry of Health and Labor and Welfare, from the Japanese Health Sciences Foundation, and from the Promotion and Mutual Aid Corporation for Private Schools of Japan.

References

1. Takahashi H. Antigen processing and presentation. *Microbiol Immunol* 1993: **37**: 1–9.
2. Porcelli SA, Segelke BW, Sugita M, Wilson IA, Brenner MB. The CD1 family of lipid antigen-presenting molecules. *Immunol Today* 1998: **19**: 362–8.
3. Takahashi H. Antigen presentation in vaccine development. *Comp Immunol Microbiol Infect Dis* 2003: **26**: 309–28.
4. Nijman HW, Kleijmeer MJ, Ossevoort MA et al. Antigen capture and major histocompatibility class II compartments of freshly isolated and cultured human blood dendritic cells. *J Exp Med* 1995: **182**: 163–74.
5. Burdin N, Kronenberg M. CD1-mediated immune responses to glycolipids. *Curr Opin Immunol* 1999: **11**: 326–31.
6. Brigl M, Brenner MB. CD1: antigen presentation and T cell function. *Annu Rev Immunol* 2004: **22**: 817–90.
7. Gumperz JE, Brenner MB. CD1-specific T cells in microbial immunity. *Curr Opin Immunol* 2001: **13**: 471–8.
8. Moody DB, Young DC, Cheng TY et al. T cell activation by lipopeptide antigens. *Science* 2004: **303**: 527–31.
9. Sieling PA, Chatterjee D, Porcelli SA et al. CD1-restricted T cell recognition of microbial lipoglycan antigens. *Science* 1995: **269**: 227–30.
10. Moody DB, Reinhold BB, Guy MR et al. Structural requirements for glycolipid antigen recognition by CD1b-restricted T cells. *Science* 1997: **278**: 283–6.
11. Beckman EM, Porcelli SA, Morita CT, Behar SM, Furlong ST, Brenner MB. Recognition of a lipid antigen by CD1-restricted alpha beta$^+$ T cells. *Nature* 1994: **372**: 691–4.
12. Moody DB, Ulrichs T, Muhlecker W et al. CD1c-mediated T-cell recognition of isoprenoid glycolipids in *Mycobacterium tuberculosis* infection. *Nature* 2000: **404**: 884–8.
13. Joyce S, Woods AS, Yewdell JW et al. Natural ligand of mouse CD1d1: cellular glycosylphosphatidylinositol. *Science* 1998: **279**: 1541–4.
14. Kawano T, Cui J, Koezuka Y et al. CD1d-restricted and TCR-mediated activation of Valpha14 NKT cells by glycosylceramides. *Science* 1997: **278**: 1626–9.
15. Exley M, Garcia J, Balk SP, Porcelli S. Requirements for CD1d recognition by human invariant Valpha24$^+$ CD4$^-$CD8$^-$ T cells. *J Exp Med* 1997: **186**: 109–20.
16. Bendelac A, Lantz O, Quimby ME, Yewdell JW, Bennink JR, Brutkiewicz RR. CD1 recognition by mouse NK1$^+$ T lymphocytes. *Science* 1995: **268**: 863–5.
17. Jayawardena-Wolf J, Bendelac A. CD1 and lipid antigens: intracellular pathways for antigen presentation. *Curr Opin Immunol* 2001: **13**: 109–13.
18. Couedel C, Peyrat MA, Brossay L et al. Diverse CD1d-restricted reactivity patterns of human T cells bearing 'invariant' AV24BV11 TCR. *Eur J Immunol* 1998: **28**: 4391–7.
19. Matsuura A, Takayama S, Kinebuchi M et al. RT1.P, rat class Ib genes related to mouse TL: evidence that CD1 molecules but not authentic TL antigens are expressed by rat thymus. *Immunogenetics* 1997: **46**: 293–306.
20. Balk SP, Bleicher PA, Terhorst C. Isolation and characterization of a cDNA and gene coding for a fourth CD1 molecule. *Proc Natl Acad Sci USA* 1989: **86**: 252–6.
21. Balk SP, Bleicher PA, Terhorst C. Isolation and expression of cDNA encoding the murine homologues of CD1. *J Immunol* 1991: **146**: 768–74.
22. Katabami S, Matsuura A, Chen HZ, Imai K, Kikuchi K. Structural organization of rat CD1 typifies evolutionarily conserved CD1D class genes. *Immunogenetics* 1998: **48**: 22–31.
23. Kashiwase K, Kikuchi A, Ando Y et al. The CD1d natural killer T-cell antigen presentation pathway is highly conserved between humans and rhesus macaques. *Immunogenetics* 2003: **54**: 776–81.
24. Shinya E, Owaki A, Shimizu M et al. Endogenously expressed HIV-1 nef down-regulates antigen-presenting molecules, not only class I MHC but also CD1a, in immature dendritic cells. *Virology* 2004: **326**: 79–89.
25. Ichikawa M, Sugita M, Takahashi M et al. Breast milk macrophages spontaneously produce granulocyte-macrophage colony-stimulating factor and differentiate into dendritic cells in the presence of exogenous interleukin-4 alone. *Immunology* 2003: **108**: 189–95.
26. Calabi F, Jarvis JM, Martin L, Milstein C. Two classes of CD1 genes. *Eur J Immunol* 1989: **19**: 285–92.
27. Stadler J, Lemmens R, Nyhammar T. Plasmid DNA purification. *J Gene Med* 2004: **6**: S54–66.
28. Zeng Z, Castano AR, Segelke BW, Stura EA, Peterson PA, Wilson IA. Crystal structure of mouse CD1: an MHC-like fold with a large hydrophobic binding groove. *Science* 1997: **277**: 339–45.
29. Beer BE, Bailes E, Goeken R et al. Simian immunodeficiency virus (SIV) from sun-tailed monkeys (*Cercopithecus solatus*): evidence for host-dependent evolution of SIV within the *C. lhoesti* superspecies. *J Virol* 1999: **73**: 7734–44.
30. Puissant B, Abbal M, Blancher A. Polymorphism of human and primate RANTES, CX3CR1, CCR2 and CXCR4 genes with regard to HIV/SIV infection. *Immunogenetics* 2003: **55**: 275–83.
31. Zajonc DM, Cantu C III, Mattner J et al. Structure and function of a potent agonist for the semi-invariant natural killer T cell receptor. *Nat Immunol* 2005: **6**: 810–8.
32. Moody DB, Zajonc DM, Wilson IA. Anatomy of CD1-lipid antigen complexes. *Nat Rev Immunol* 2005: **5**: 387–99.
33. Giabbai B, Sidobre S, Crispin MD et al. Crystal structure of mouse CD1d bound to the self ligand phosphatidylcholine: a molecular basis for NKT cell activation. *J Immunol* 2005: **175**: 977–84.
34. Koch M, Stronge VS, Shepherd D et al. The crystal structure of human CD1d with and without alpha-galactosylceramide. *Nat Immunol* 2005: **6**: 819–26.
35. Kim Y, Nakagawa Y, Sugiyama H et al. Induction of CD4$^+$ murine natural killer T-like cells by immunization with syngeneic thymoma expressing embryonic alpha-fetoprotein. *Cell Immunol* 2003: **226**: 1–10.

36. Kojo S, Adachi Y, Keino H, Taniguchi M, Sumida T. Dysfunction of T cell receptor AV24AJ18^{+}, BV11^{+} double-negative regulatory natural killer T cells in autoimmune diseases. *Arthritis Rheum* 2001: **44**: 1127–38.
37. Hansen DS, Schofield L. Regulation of immunity and pathogenesis in infectious diseases by CD1d-restricted NKT cells. *Int J Parasitol* 2004: **34**: 15–25.
38. Cranage MP, Cook N, Stott EJ, Cook R, Baskerville A, Greenaway PJ. Transmission studies with simian immunodeficiency virus of macaques; persistent infection of baboons. *Intervirology* 1992: **34**: 53–61.
39. Huet T, Cheynier R, Meyerhans A, Roelants G, Wain-Hobson S. Genetic organization of a chimpanzee lentivirus related to HIV-1. *Nature* 1990: **345**: 356–9.

J Med Primatol 2005: 34: 294–302

JOURNAL OF MEDICAL PRIMATOLOGY

Early virological events in various tissues of newborn monkeys after intrarectal infection with pathogenic simian human immunodeficiency virus

Miyake A, Ibuki K, Suzuki H, Horiuchi R, Saito N, Motohara M, Hayami M, Miura T. Early virological events in various tissues of newborn monkeys after intrarectal infection with pathogenic simian human immunodeficiency virus. J Med Primatol 2005; 34:294–302.

Ariko Miyake, Kentaro Ibuki, Hajime Suzuki, Reii Horiuchi, Naoki Saito, Makiko Motohara, Masanori Hayami, Tomoyuki Miura

Institute for Virus Research, Kyoto University, Kyoto, Japan

Key words: early phase of infection – immature T cells – newborn monkey – SHIV – thymus

Accepted April 25, 2005.

Tomoyuki Miura DVM PhD, Laboratory of Primate Model, Experimental Research Center for Infectious Disease, Institute for Virus Research, Kyoto University, Sakyo-ku, Kyoto, 606-8507, Japan. Tel.: 81 75 751 3981; fax: 81 75 761 9335; e-mail: tmiura@virus.kyoto-u.ac.jp

Funding: This work was supported by a Health Sciences Research Grant from the Ministry of Health, Labour and Welfare, Japan and a Grant-in-Aid for Scientific Research from the Ministry of Education and Science, Japan. A. M. is a recipient of a Research Resident Fellowship for junior researchers of the Japanese Foundation for AIDS Prevention.

Abstract: Children infected with human immunodeficiency virus type 1 often have higher viral loads and progress to acquired immunodeficiency syndrome more rapidly than adults. In our previous study of simian–human immunodeficiency virus (SHIV)-infected adult monkeys, immature CD4CD8 double-positive T cells in the thymus and jejunum decreased faster than mature CD4 single-positive T cells. Here, we examined the effect of virus replication on immature T cells from the same SHIV-inoculated newborn monkeys having more immature T cells than adults. The infectious viruses were more abundantly detected in the thymus than in other tissues at both 13 and 26 days post-infection (dpi). However, mature $CD4^+$ T cells in the thymus declined after 13 dpi and immature $CD3^-$ CD4 single-positive T cells remained at 26 dpi. These results suggested that many immature $CD4^+$ T cells in the thymus of newborns support the production of infectious viruses even after the depletion of mature $CD4^+$ T cells.

Introduction

Children infected with human immunodeficiency virus type 1 (HIV-1) often have higher viral loads and progress to AIDS more rapidly than adults [2, 8, 20]. In the absence of antiretroviral treatments, the disease progresses rapidly, with up to 45% of infected children developing AIDS and dying within the first 2 years of life [Joint United Nations Programme on HIV/AIDS (UNAIDS), 2002], while adults with HIV-1 infection have an asymptomatic period for 10 or more years. The reason for the rapid progression and high viral loads in newborns is unclear. The advanced stage of disease has generally been attributed to the immaturity of the immune system. However, children are reported to have active cellular and humoral immune responses to HIV infection [12, 23]. Moreover, in a study using the simian immunodeficiency virus (SIV)-macaque monkey model, Veazey et al. [22] showed that newborn monkeys have more activated T cells in the intestinal tract and that activated cells were the source of high viral load and the rapid progression to AIDS.

In our previous study using adult macaque monkeys, we observed that the percentage of CD4CD8 double positive (DP) T cells was much higher in the thymus and intestinal tract than in other tissues examined [Miyake A, Ibuki K, Enose Y, Suzuki H, Horiuchi R, Suzuki M, Saito N, Nakasone T, Honda M, Watanabe T, Miura T, Hayami M, unpublished data]. Both tissues were reported as sites of maturation of lymphocytes [4, 10], and CD4CD8 DP T cells have been proposed to represent immature stages in T cell development. These immature CD4CD8 DP T cells decreased earlier than mature CD4 single positive (SP) T cells in the thymus and jejunum after infection of a

pathogenic SIV/HIV-1 chimeric virus [simian–human immunodeficiency virus (SHIV)]. These results suggested that the rate of virus replication is greater in immature T cells than in mature T cells. Newborns have more immature T cells than adults [5, 13], which might contribute to the higher rate of disease progression in newborns.

In this study, we analyzed newborn monkeys infected with the SHIV that were used in the study with adult monkeys [Miyake A, Ibuki K, Enose Y, Suzuki H, Horiuchi R, Suzuki M, Saito N, Nakasone T, Honda M, Watanabe T, Miura T, Hayami M, unpublished data], and compared the results in newborn and adult monkeys. In newborns examined at both 13 and 26 days after inoculation, infectious viruses were more abundant in the thymus than in other tissues. In the lymphoid tissues except the thymus, $CD4^+$ T cells were more rapidly and profoundly depleted in newborns than in adults. Moreover, not many $CD4^+$ T cells were present in the intestinal tracts of newborns, even in the uninfected control. However, in the thymus of newborns, there were many $CD4^+$ T cells including mature and immature $CD4^+$ T cells at 13 days after inoculation, and immature $CD3^-$ $CD4^+$ T cells remained even after the depletion of mature $CD4^+$ T cells.

Materials and Methods

Virus

The SHIV-C2/1 was generated by *in vivo* passage of SHIV-89.6 (containing env, tat, rev and vpu derived from primary isolates of HIV-1) [17]. SHIV-C2/1 KS661c is a molecular clone, which was constructed from the consensus sequence of SHIV-C2/1 (GenBank accession number AF217181). SHIV-C2/1 KS661c can infect macaque monkeys by intravenous and intrarectal routes and cause precipitous viremia and drastic $CD4^+$ cells depletion. The virus stock was prepared from supernatant of a human lymphoid cell line, CEMx174, and stored in liquid nitrogen (−190°C) until use. The 50% tissue culture infectious dose ($TCID_{50}$) of the virus stock was measured in CEMx174. Twenty $TCID_{50}$ was equivalent to one 50% macaque infectious dose (MID_{50}).

Monkeys and virus inoculation

Three newborn rhesus macaques (*Macaca mulatta*) were used in this study. All monkeys used in this study were treated in accordance with the institutional regulations approved by the Committee for Experimental Use of Nonhuman Primate in the Institute for Virus Research, Kyoto University. Two monkeys were anesthetized by intramuscular injection of ketamine chloride and inoculated intrarectally with 2×10^3 $TCID_{50}$ of SHIV-C2/1 KS661c. All intrarectal inoculations were performed with a pediatric feeding catheter inserted a distance of 5 cm from the anus. The catheter was inserted carefully to avoid causing trauma. The inoculated monkeys were killed at 13 and 26 days after inoculation, respectively. The third monkey was not inoculated and was used as a normal control.

Sample collection

Prior to killing, blood was collected from the inguinal vein under ketamine anesthesia. Intravenous pentobarbital (Nembutal; Abbott Laboratories, Abbott Park, IL, USA) (40 mg/kg) was administered for deeper anesthesia. After thoracotomy, the right atrium was incised, and 500 ml of sterile heparinized saline (5 U/ml) was infused into the left ventricle using an 18-gauge needle attached to infusion tubing. After the perfusion, complete sets of organs were obtained for the following analyses. Peripheral blood mononuclear cells (PBMC) and plasma were separated from heparinized blood by Percoll (Lymphocyte Separation Solution; Nacalai Tesque, Kyoto, Japan) density gradient centrifugation. Plasma was frozen at −80°C until used. Parts of the organ samples were frozen directly at −80°C until used for quantification of proviral DNA. Residual samples of spleen, thymus and axillary, inguinal and mesenteric lymph nodes were minced and filtered through a 40 μm nylon filter (Becton Dickinson, Franklin Lakes, NJ, USA). Samples of jejunum were washed in Dulbecco's Modified Eagle's Medium (DMEM) containing 0.45 mM DTT, cut into 1-cm^2 pieces and agitated in DMEM medium containing 5% fetal calf serum (FCS) for 1 hour at room temperature (RT). After a short sedimentation, supernatants and tissue fragments were processed to give intraepithelial lymphocytes (IEL) and lamina propria lymphocytes (LPL), respectively. The supernatants (containing IEL) were filtered through columns containing packed glass wool and centrifuged at 1600 rpm for 7 minute. The pellets were suspended in 30% Percoll (Pharmacia, Uppsala, Sweden) and centrifuged at 1800 rpm for 20 minute. The pellets were resuspended in 44% Percoll, layered on 70% Percoll and centrifuged at 1800 rpm for 20 minute. Cells at the interface between the 44 and 70% Percoll layers were collected. The residual tissue fragments were agitated in Hanks buffer containing 5 mM EDTA for 10 minutes at RT, and the supernatants were removed. This step was repeated three times. The